Biochemical Pharmacology xxx (xxxx) xxxx

Contents lists available at ScienceDirect

Biochemical Pharmacology

journal homepage: www.elsevier.com/locate/biochempharm

Correction of arginine metabolism with sepiapterin—the precursor of nitric oxide synthase cofactor BH_4—induces immunostimulatory-shift of breast cancer

Xunzhen Zheng[1], Veani Fernando[1], Vandana Sharma[1], Yashna Walia, Joshua Letson, Saori Furuta*

Department of Cancer Biology, College of Medicine and Life Sciences, University of Toledo Health Science Campus, 3000 Arlington Ave., Toledo, OH 43614, USA

ARTICLE INFO

Keywords:
Arginine metabolism
Breast cancer
Tumor-associated macrophages
Macrophage reprogramming
Nitric oxide

ABSTRACT

Immunotherapy is a first-line treatment for many tumor types. However, most breast tumors are immunosuppressive and only modestly respond to immunotherapy. We hypothesized that correcting arginine metabolism might improve the immunogenicity of breast tumors. We tested whether supplementing sepiapterin, the precursor of tetrahydrobiopterin (BH_4)—the nitric oxide synthase (NOS) cofactor—redirects arginine metabolism from the pathway synthesizing polyamines to that of synthesizing nitric oxide (NO) and make breast tumors more immunogenic. We showed that sepiapterin elevated NO but lowered polyamine levels in tumor cells, as well as in tumor-associated macrophages (TAMs). This not only suppressed tumor cell proliferation, but also induced the conversion of TAMs from the immuno-suppressive M2-type to immuno-stimulatory M1-type. Furthermore, sepiapterin abrogated the expression of a checkpoint ligand, PD-L1, in tumors in a STAT3-dependent manner. This is the first study which reveals that supplementing sepiapterin normalizes arginine metabolism, improves the immunogenicity and inhibits the growth of breast tumor cells.

1. Introduction

Immunotherapy has become an effective means to attack many types of cancers. However, the majority (88–90%) of breast tumors only modestly respond to common immunotherapy, especially those using anti-PD-L1 antibodies [1]. These tumors are immuno-suppressive, infiltrated by large populations of regulatory T (Treg) cells and M2-type tumor-associated macrophages (TAMs) that dampen the activity of cytotoxic T cells [2–4]. While half of ongoing trials for breast tumor immunotherapy are still testing PD-1/PD-L1-targeted drugs [2,3,5–8], it is imperative to develop a novel treatment to help improve the immunogenicity of breast tumors.

TAM-targeted immunotherapies have recently been explored as a means to improve the immunogenicity of tumors [9]. TAMs include tumoricidal M1-type and pro-tumoral M2-type. M1 TAMs are induced by Th1-type stimuli that activate nitric oxide synthase 2 (NOS-2) to produce NO from arginine, triggering pro-inflammatory signals [10]. In contrast, M2 TAMs are induced by Th2-type stimuli that activate arginase 1 (ARG1) to initiate polyamine synthesis from arginine, triggering anti-inflammatory signals [10]. Lowered M1/M2 TAM ratio often accounts for the immunotherapy-refractoriness of tumors [11,12]. To improve the M1/M2 TAM ratio, different methods to reprogram M2-TAMs to M1-TAMs have been actively investigated [9]. Nevertheless, most studies utilize pro-inflammatory agents (e.g., LPS, IFN-γ, or TNFα) or activators of the signaling pathways (e.g., agonists for Toll-like receptor (TLR) or CD40) [9–12]. Such methods could not only induce adverse side effects (e.g., septic shock by LPS or IFN-γ and liver toxicity by CD40 or TLR agonists) if used *in vivo* [13–16], but also exert dichotomous effects as both anti- and pro-tumor agents [17–20]. To move this field forward, it is essential to devise an alternative approach that improves the M1/M2 TAM ratio with potent anti-tumor activities and little side effects.

We hypothesized that correction of arginine metabolism, which is often altered in tumors [21], would improve the immunogenicity of breast tumors and suppress their growth. To this end, we sought to replenish the cofactors of arginine metabolic pathways diminished in tumors, which would exert minimal side effects. Arginine is metabolized into multiple products. Among these, the major pathways are those of producing NO, a gaseous signaling molecule (Red in Fig. 1), and polyamines, small polycationic metabolites (Green in Fig. 1)

* Corresponding author.
E-mail address: Saori.Furuta@utoledo.edu (S. Furuta).
[1] These authors contributed equally to the work.

https://doi.org/10.1016/j.bcp.2020.113887
Received 11 October 2019; Accepted 24 February 2020

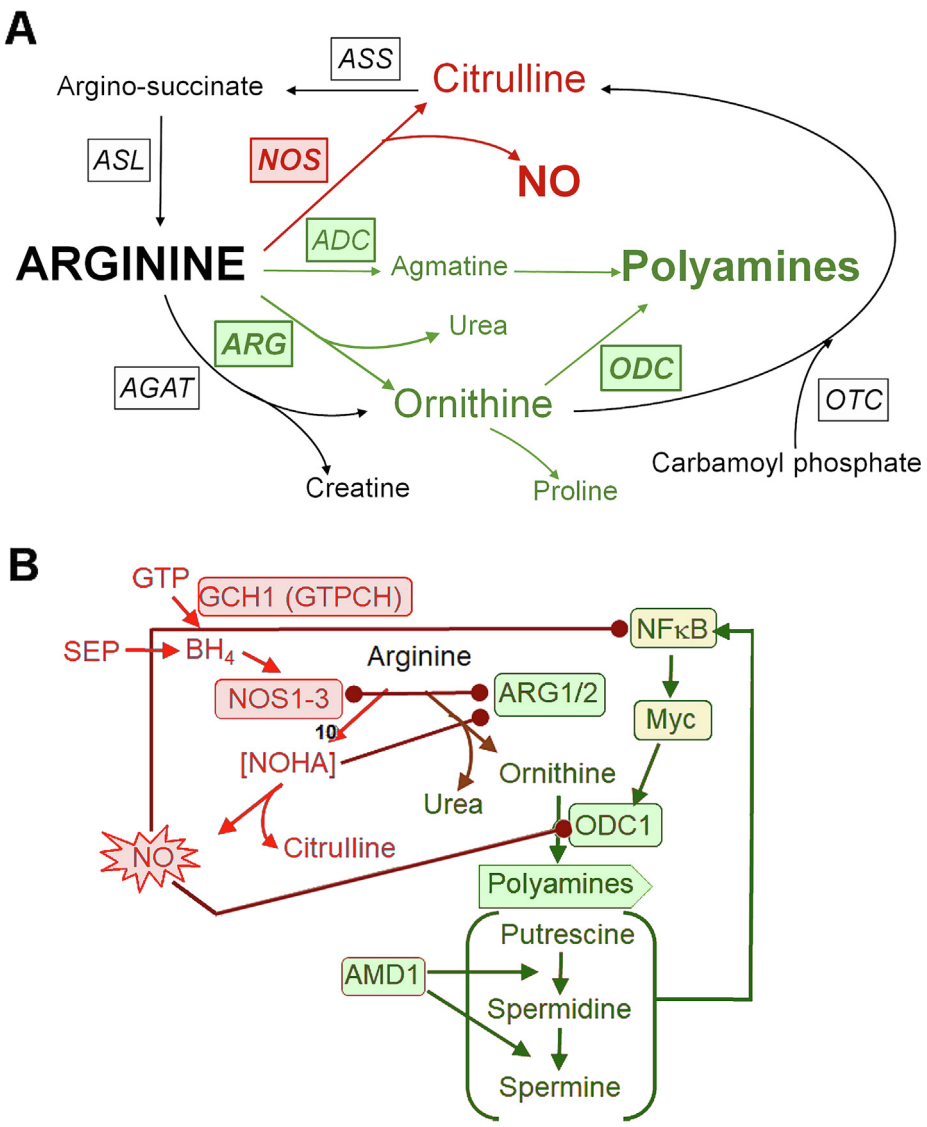

Fig. 1. Two major arginine metabolic pathways: NO synthesis vs. polyamine synthesis pathways. A) Arginine metabolic pathways: NO synthesis pathway is shown in red, while polyamine synthesis pathways are shown in green. B) Antagonistic relationship between NO and polyamine synthesis pathways. Abbreviations: ADC: Arginine decarboxylase; AGAT: Arginine:glycine amidinotransferase; AMD1: Adenosylmethionine decarboxylase 1; ARG1/2: Arginase 1/2; ASL: Argininosuccinate lyase; ASS; BH_4: tetrahydrobiopterin; GCH1: GTP cyclohydrolase I; GTP: Guanosine-5′-triphosphate; NO: nitric oxide; NFκB: Nuclear factor kappa B; Myc: Avian myelocytomatosis viral oncogene; NOS1-3: nitric oxide synthase 1–3; ODC1: Ornithine decarboxylase 1; OTC: Ornithine transcarbamylase; SEP: Sepiapterin.

[22,23]. NO and polyamine signaling counteract each other. For example, NO triggers Th1-type pro-inflammatory signals (e.g., M1-type macrophages), whereas polyamines trigger Th2-type anti-inflammatory signals (e.g., M2-type macrophages) [24]. Furthermore, NO vs. polyamine synthesis pathways inhibit each other [25–29]. In tumor cells and tumor-infiltrating immune cells, such as TAMs, arginine metabolism is frequently shunted into polyamine synthesis pathway, promoting cell proliferation and immuno-suppression [21,26–28,30–33].

We tested whether supplementing sepiapterin, an endogenously-produced precursor of the NOS cofactor BH_4 (14), could redirect arginine metabolism from the pathway synthesizing polyamines to that of synthesizing NO in mammary tumors. BH_4 plays essential roles in the formation of the functional dimer, substrate binding and enzymatic functions of NOS [34–36]. We previously reported that BH_4 bioavailability in breast epithelial cells declined during early-stage carcinogenesis, lowering basal NO production. Treating cultured breast cancer cells with sepiapterin not only normalized basal NO levels, but also suppressed cell proliferation [37–39].

In the present study, we examined whether sepiapterin could suppress the growth of mammary tumors and improve the immunogenicity using *ex vivo* 3D culture models. We found that sepiapterin efficiently shifted arginine metabolism from polyamine synthesis to NO synthesis pathways in mammary tumor cells and TAMs. This suppressed cell proliferation and expression of PD-L1, a checkpoint inhibitor, in tumor cells in a manner dependent on STAT3 activity. Concomitantly, sepiapterin caused conversion of M2-type TAMs to M1-type TAMs, further improving the immunogenicity of tumors. This study, for the first time, reveals that sepiapterin normalizes arginine metabolism, improves immunogenicity and inhibits the growth of mammary tumors.

2. Materials & methods

2.1. Reagents

For inhibition of NO production, cells were treated with 2.5 mM L-NAME (N_ω-Nitro-L-arginine methyl ester hydrochloride, Sigma-Aldrich, St. Louis, MO, USA); for induction of NO production, 2.5 μM SNAP (S-Nitroso-N-acetyl-DL-penicillamine, Sigma-Aldrich) or 2.5 μM GSNO (S-nitrosoglutathione, Sigma-Aldrich) was used. To inhibit ODC1, the rate-limiting enzyme of polyamine synthesis, DMFO (DL-α-Difluoromethylornithine, Sigma-Aldrich) was used at 5 mM. To compensate for the reduced BH_4 level in cancer cells and M2-type macrophages, 20 or 100 μM L-sepiapterin (BH_4 precursor, Sigma-Aldrich or Santa Cruz Biotech. (Santa Cruz, CA, USA)) was used. For iNOS inhibition, iNOS inhibitor (1400 W) was obtained from Cayman Chemical (Ann Arbor, MI, USA) and used at 50 and 100 μM for 2 days [40]. For inhibition of STAT3, 2.5 μM Stattic (Tocris Biosci., Minneapolis, MN, USA) was used. For inhibition of SMAD3, 25 μM SIS3 (Sigma-Aldrich)

was used. For macrophage differentiation/polarization, 100 ng/ml phorbol 12-myristate 13-acetate (PMA, Invivogen, San Diego, CA, USA), 5 ng/ml lipopolysaccharide (LPS, Sigma-Aldrich), 20 ng/ml Interferon-γ (IFN-γ, PeproTech, Rocky Hill, NJ, USA), 20 ng/ml interleukin-4 (IL-4, PeproTech) and 20 ng/ml interleukin-13 (IL-13, PeproTech) were used.

2.2. Antibodies

To determine the expression of target proteins, the following antibodies were used. Anti-CD163 (Abcam, Cambridge, MA, USA, ab182422), anti-CD80 (ThermoFisher Sci., MA5-15512), anti-iNOS (ThermoFisher Sci., PA1-036); anti-Stat1 (Cell Signaling, 9172 T), anti-p-Stat1 (Tyr701, Cell Signaling, 7649 T), anti-STAT3 (Cell Signaling, 9139 T), anti-p-Stat3 (Ser727, ThermoFisher Sci., 44-384G), anti-IL-12 (R&D, AF309-SP), anti-IL-10 (R&D, AF217-SP), anti-p-Smad3 (Novus Bio, Centennial, CO, USA, nbp1-77836), anti-PD-L1 (Abcam, ab205921, for western blot), anti-PD-L1 polyclonal antibody (Biorbyt, LLC, San Francisco, CA, USA, orb74809, for IHC), anti-β-Actin (Sigma-Aldrich, A1978); anti-mouse CK 8/18 (DSHB, Iowa City, IA, USA, Troma-I); anti-mouse CK 14 (BioLegend, San Diego, CA, USA, 905301); and anti-mouse F4/80 (eBioscience, Waltham, MA, USA, BM8).

2.3. Cell lines and cell culture

CA1d human breast cancer cells were obtained from Karmanos Cancer Institute (Detroit, MI, USA) [41] under Material Transfer Agreement. THP-1 human monocytic cells were obtained from American Tissue Culture Collection (ATCC, Manassas, VA, USA). These cell lines had been authenticated by the providers through genome sequencing and STR profiling. Mycoplasma testing of these cell lines was negative. CA1d breast cancer cells were maintained as described [41]. THP-1 cells were maintained at a cell density of 1×10^5/ml–1×10^6/ml in RPMI 1640 supplemented with 10% FBS, 2 mM L-glutamine, 10 mM HEPES buffer and 1% penicillin/streptomycin as described (All purchased from ThermoFisher Sci., Waltham, MA, USA) [42,43]. All cells were maintained in a 37 °C humidified incubator with 5% CO_2.

2.4. In vitro macrophage polarization

THP-1 cells were subjected to differentiation followed by M1 vs. M2 polarization as described [44]. Briefly, cells were seeded in 24-well plates at a density of 250,000 cells/ml. To differentiate monocytic THP-1 cells to macrophages, cells were treated with 100 ng/ml PMA for 24 h. To obtain M1-polarized macrophages, 5 ng/ml LPS and 20 ng/ml IFN-γ were added to PMA-treated cells, and cells were maintained for up to 66 h. To obtain M2-polarized macrophages, 20 ng/ml IL-4 and 20 ng/ml IL-13 were added to PMA-treated cells, and cells were maintained for up to 66 h. For macrophage reprogramming experiment, 20 or 100 μM sepiapterin was added to M2-polarized macrophages, and cells were maintained for 2 days. Medium was unchanged throughout the entire differentiation/polarization/reprogramming experiment.

2.5. Nitrite measurement

To quantify the cumulative level of nitric oxide produced by cells, more stable nitric oxide metabolite, nitrite, was measured based on the reaction of a dye DAN (2, 3– diaminonaphthalene) by using Nitric Oxide Fluorometric Assay Kit (BioVision, Inc, Milpitas, CA, USA, #K252) according to the manufacturer's protocol. Briefly, cells were plated at 250,000 cells/ml in a 24-well plate and subjected to drug treatment (cancer cells) or differentiation, polarization and reprogramming (macrophages). Cells were maintained in 2 ml of the fresh serum free hematopoietic cell medium (phenol red-free, Lonza, Basel, Switzerland, #04-744Q) throughout the experiment. The conditioned medium was harvested and 10 μl of the medium was reacted with the assay reagents in the dark, and the signal intensity was measured using nitrite standards at the fluorescence wavelengths of Ex/Em = 360/450 nm.

2.6. Polyamine measurement

To determine polyamine levels produced by cells, conditioned media were analyzed with Fluorometric Total Polyamine Assay Kit (BioVision, # K475) according to the manufacturer's protocol with modifications. This kit determines the level of hydrogen peroxide produced through oxidation of polyamines by spermine/spermidine oxidase in the kit. To remove high background levels of hydrogen peroxide produced by cancer cells and macrophages prior to the assay, the conditioned media were pretreated with catalase (Sigma-Aldrich or Novus Bio) at 1 U/ml (for cancer cells) or 100 μg/ml (for macrophages) and incubated at 37 °C for 1 h (for cancer cells) or 1.5 h (for macrophages). Proteins were precipitated with Sample Clean-up Solution provided by the kit, and the precipitated proteins were removed by filtration through 10 kDa cut-off Microcon filter (Millipore, St. Louis, MO, USA). The flow through was reacted with the assay reagents in the dark, and the signal intensity was measured using polyamine standards at the fluorescence wavelengths of Ex/Em = 535/587 nm.

2.7. Ex vivo 3D cultures of mouse mammary tumors

All animal experiments conformed to The Guide for the Care and Use of Laboratory Animals (National Research Council, National Academy Press, Washington, D.C., 2010) and were performed with the approval of the Institutional Animal Care and Use Committee of the University of Toledo, Toledo, OH. Mouse mammary tumors (#4 glands, ~ 1 cm in diameter, n = 4) were harvested from 18 weeks old female MMTV-PyMT mice (The Jackson Laboratory, Bar Harbor, ME, USA). Tumors were rinsed in PBS and chopped into ~1 mm × 2 mm × 1 mm fragments, as previously described [45,46]. 1–2 fragments/48 well were plated onto the ECM gel coat (Matrigel, Corning, Corning, NY, USA) and cultured in HMT-3522 S1 medium [47,48] with 4% Matrigel and sepiapterin (0, 20 or 100 μM) for one week with drug replenishment every 2–3 days. Tumors were fixed, paraffin-embedded, sectioned and stained with eosin/hematoxylin.

2.8. Immunohistochemistry

To determine the expression of specific markers, paraffin-embedded sections of mouse mammary tissues were analyzed by immunohistochemistry. Briefly, sections were deparaffinized, hydrated, and treated with antigen unmasking solution (Vector Lab., Inc., Burlingame, CA, USA) or with Tris-EDTA Buffer (10 mM Tris Base, 1 mM EDTA Solution, 0.05% Tween 20, pH 9.0) which had been heated to 95–100 °C in a pressure cooker. After being blocked with nonimmune goat serum, sections were processed for immunofluorescence staining as described below.

2.9. Immunofluorescence staining and imaging

Immunofluorescence staining/imaging was performed as described previously [37]. Samples were incubated with primary antibody for overnight at 4 °C in a humidified chamber. After intensive washing (three times, 15 min each) in 0.1% BSA, 0.2% Triton-X 100, 0.05% Tween 20, 0.05% NaN3 in PBS, fluorescence-conjugated secondary antibodies (Molecular Probes, Waltham, MA, USA) were added for 2 h at room temperature. Nuclei were stained with 0.5 ng/ml DAPI. After mounted with anti-fade solution, epi-fluorescence imaging was performed on Olympus IX70 microscope using CellSens software. Confocal fluorescence imaging was performed on Leica Microsystems TCS SP5 multi-photon laser scanning confocal microscope using Suite Advanced Fluorescence (LAS AF) software.

2.10. Image analysis

Quantification of fluorescence signal in micrographs was performed with ImageJ software (NIH) referring to the owner's manual (http://imagej.net/docs/guide/146.html). Briefly, a region of interest (ROI) was determined in reference to an image of DAPI-stained nuclei. For quantification of signal in individual cultured cells, the whole cell was selected as ROI. For each sample group, at least 50 to 200 measurements were performed. Furthermore, measurement of each sample set was repeated by at least three people, and the results were combined for the final data. The mean value was represented as arbitrary units (AU). The statistical significance of the data was further evaluated using GraphPad Prism Version 5 software (see statistics section).

2.11. Statistics

All the experiments were performed in replicates ($n >= 3$ for *in vitro* experiments; $n > 6$ for *ex vivo* experiments) ensuring the adequate statistical power as done previously [49]. Unless otherwise indicated, statistical significance of the mean difference was tested by two-tailed t-tests (parametric) using GraphPad Prism Version 5 software. P-values of 0.05 or less were considered significant. Average results of multiple experiments ($n >= 3$) are presented as the arithmetic mean ± SEM.

3. Results

3.1. Sepiapterin promotes basal NO production, while suppressing polyamine synthesis, in breast cancer cells and macrophages

In tumors, arginine metabolism is frequently shunted from NO synthesis to polyamine synthesis pathways, promoting the growth and immuno-suppressive nature (Fig. 1A) [21,26–28,30–33]. These two pathways are reported to antagonize each other not only for their syntheses, but also for their downstream signaling (Fig. 1B) [22–29,50–54]. Polyamine facilitates the activities of the immuno-suppressive M2-type TAMs, impairing the pro-inflammatory M1-type TAMs. Conversely, NO facilitates the immuno-stimulatory activities of M1-type TAMs, inhibiting M2-type TAMs [55,56]. Normalizing arginine metabolism is expected to improve the immunogenicity and suppress the growth of tumors.

We recently reported that breast epithelial cells produce basal NO when cultivated in the basement membrane. Conversely, the production is impaired in cells undergoing the early-stage breast carcinogenesis, resulting in the upregulation of TGFβ and HER2 [37–39]. The declined basal NO production is due to reduced bioavailability of the NOS cofactor, BH_4, under oxidative stress. Consistently, ectopic addition of the BH_4 precursor, sepiapterin, restores basal NO production and inhibits proliferation of breast cancer cells [39].

In the present study, we tested our hypothesis that these effects of sepiapterin are due to the fact that it could re-direct arginine metabolism from polyamine synthesis to NO synthesis pathways. We treated CA1d breast cancer cells with sepiapterin at 20 or 100 μM for three days and measured the levels of NO vs. polyamines (Fig. 2A). As a positive control, cells were treated with an NO donor, SNAP (2.5 μM) or GSNO (2.5 μM). As a negative control, cells were treated with an NOS antagonist, L-NAME (2.5 mM). Vehicle-treated (control) cells produced slightly (1–1.2 fold) higher levels of polyamines than NO. This trend was exacerbated by L-NAME-treatment, where cells produced 1.5–2 fold higher levels of polyamines than NO. In contrast, SNAP or GSNO-treated cells produced 1.5–2 fold higher levels of NO than polyamines. Strikingly, sepiapterin-treatment increased the NO/polyamine ratio by up to 12 fold in a dose-dependent manner (Fig. 2A). This result clearly demonstrates that sepiapterin shifted arginine metabolism from polyamine synthesis to NO synthesis pathways.

Next, we tested whether sepiapterin could also influence arginine metabolism and phenotype of TAMs. M1 vs. M2-type TAMs play critical roles in determining the immunogenicity of the tumor microenvironment (TME) [57]. Consistent with a previous report [56], *in vitro*-polarized M1-type macrophages preferentially produced NO over polyamines, while M2-type macrophages preferentially produced polyamines over NO (Fig. 2B). We suspected that the difference in arginine metabolism of M1 vs. M2-types might be attributed to different bioavailability of BH_4. We searched the public database (GSE5099) [58] for the expression levels of enzymes involved in BH_4 synthesis (Fig. 3A) [59,60]. Among all, two critical enzymes, GTP cyclohydrolase (GCH1, the rate-limiting enzyme) and sepiapterin reductase (SR, the final enzyme of synthesis reactions) (Fig. 3A), were highly elevated in M1, but diminished in M2 macrophages (Fig. 3B) [61–64]. This suggests that BH_4 level is likely to be elevated in M1 and down-modulated in M2 TAMs. To test the relevance of BH_4 availability to the TAM phenotype, we provided M2 macrophages with 20 μM sepiapterin for two days. This caused a dramatic increase of NO and decrease of polyamine levels, raising the NO/polyamine ratio by ~4 fold (Fig. 2B).

Consistently, sepiapterin treatment of CD163 + M2-type macrophages led to their robust conversion to iNOS + M1-type macrophages, which was more efficient than that by lipopolysaccharide (LPS), a known inducer of the M2-to-M1 TAM conversion (Fig. 4A) [65]. To validate that sepiapterin indeed reprogrammed M2-type macrophages to M1-type macrophages, we measured a number of different markers for M1 vs. M2 macrophages. M1 macrophage markers we tested were STAT1, phospho-STAT1 (p-Y701) and IL-12; M2 macrophage markers we tested were IL-10, CD163 and STAT3 [66,67]. Especially, the production of IL-12 (Th1 cytokine) vs. IL-10 (Th2 cytokine) serves as the functional validation of M1 vs. M2 macrophages [66]. Our western blot analyses showed that sepiapterin treatment of M2-macrophages significantly elevated all the M1 markers tested, while downmodulating M2 markers. In contrast, sepiapterin did not affect the levels of M1 and M2 marker in M1 macrophages. Importantly, sepiapterin treatment of M2-macrophages increased IL-12 level by ~70%, while decreasing IL-10 level by ~70% (Fig. 4B). These results confirm that sepiapterin induced reprogramming of M2 macrophages to the functional M1 macrophages.

3.2. Sepiapterin inhibits proliferative phenotype of mammary tumor cells

To test whether sepiapterin indeed suppresses the proliferative phenotype of tumors, we applied the drug to *ex vivo* 3D-cultured mammary tumors for one week. These tumors were derived from MMTV-PyMT mice, which form multifocal, metastatic luminal B-type tumors [68]. Sepiapterin (100 μM) greatly suppressed their proliferative phenotype, indicated by diminished density of tumor epithelium (cytokeratin 14 level). Such effect of sepiapterin was in stark contrast with that of L-NAME (NOS antagonist, 2.5 mM) exacerbating the proliferative phenotype of tumors (Fig. 5A).

3.3. Sepiapterin inhibits the expression of the immune checkpoint ligand PD-L1 in mammary tumor cells via suppression of STAT3 activity

We hypothesized that this anti-tumor activity of sepiapterin was partly due to its immuno-stimulatory effects. We measured the level of an immune checkpoint ligand, PD-L1, a major executor of immunosuppression [69]. As expected, PD-L1 was highly expressed in control tumors. In contrast, sepiapterin abrogated PD-L1 expression, along with diminished density of tumor epithelium (cytokeratin 8/18 level). This was again in stark contrast with the effect of L-NAME that greatly elevated PD-L1 level (Fig. 5B).

To examine the mechanism of NO-mediated PD-L1 regulation, we tested for the involvement of STAT3 and SMAD3, known positive regulators of PD-L1 [70,71]. Besides, STAT3 and SMAD3 are shown to be negatively regulated by NO [36,39,72]. To determine which transcription factor was involved in L-NAME-induced upregulation of PD-

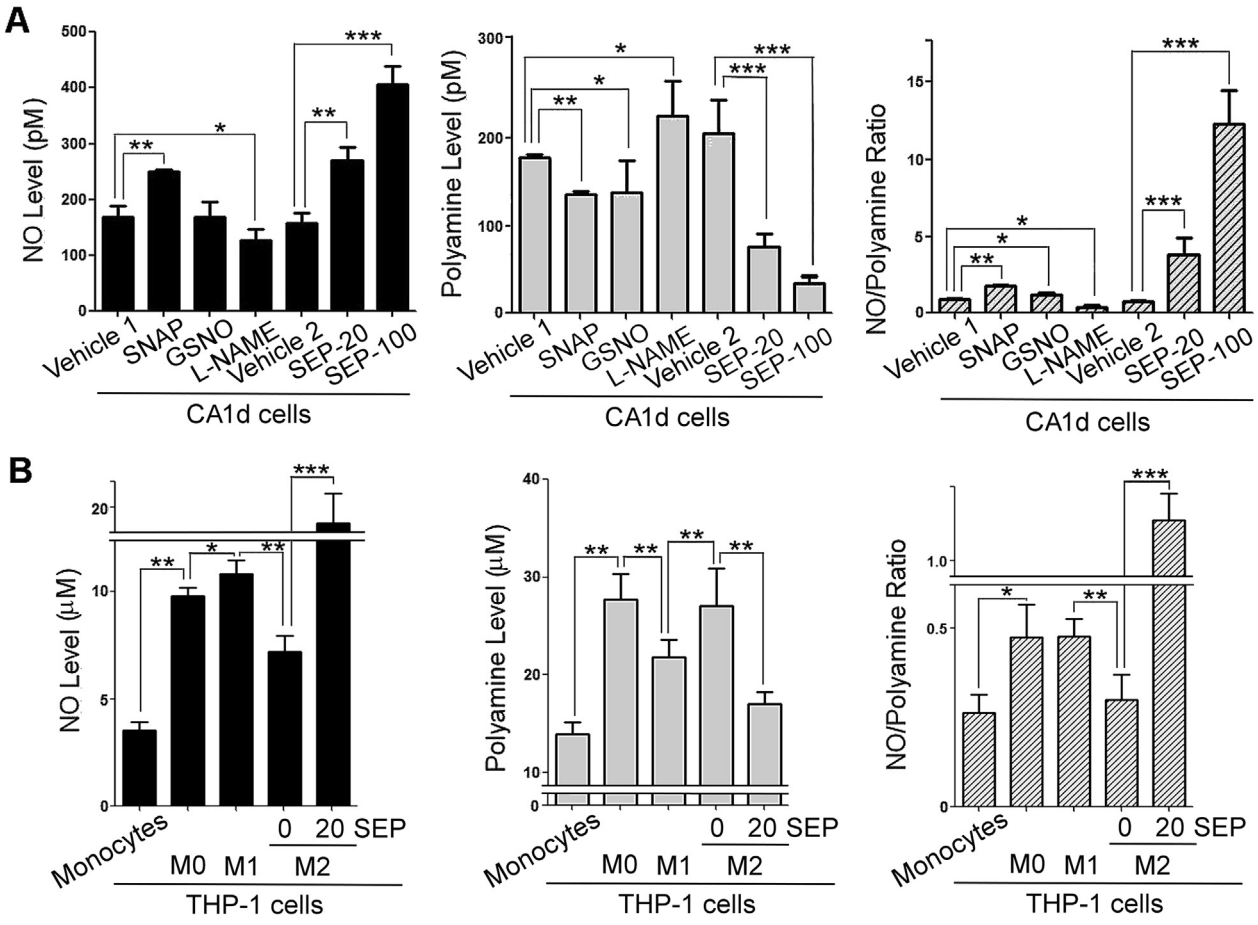

Fig. 2. Sepiapterin redirects arginine metabolism from polyamine synthesis to NO synthesis pathways in breast cancer cells and macrophages. A) Levels of NO vs. polyamines secreted by CA1d cells vehicle-treated (vehicle 1: H_2O; vehicle 2: DMSO) or treated with NO donor (SNAP [2.5 μM] or GSNO [2.5 μM]), NOS inhibitor (L-NAME [2.5 mM]) or sepiapterin (SEP, 20 or 100 μM) for 3 days. B) Levels of NO vs. polyamines secreted by *in vitro*-polarized THP-1 cells (Monocytes, M0, M1 or M2-type). M2 cells were further treated with or without sepiapterin (SEP, 20 μM) for 2 days. Error bars: ± SEM. *, p-value < 0.05; **, p-value < 0.01, ***, p-value < 0.001.

L1, we inhibited STAT3 (Stattic) or SMAD3 (SIS3) in breast cancer cells treated with L-NAME. (We confirmed the efficacy of Stattic and SIS3 in downmodulating STAT3 (p-STAT3) and SMAD3 (p-SMAD3), respectively (Fig. 6A, lanes 5, 6)). As expected, L-NAME significantly elevated PD-L1, p-STAT3 and p-SMAD3 levels (Fig. 6A, lanes 2, 10). However, L-NAME-mediated increase of PD-L1 was abrogated by STAT3 inhibition, but not by SMAD3 inhibition, suggesting the critical role of STAT3 (Fig. 6A, lanes 3, 4).

Sepiapterin, which would promote NO production, downmodulated both p-STAT3 and PD-L1 levels (Fig. 6A, lane 8). (This effect of sepiapterin was abrogated by co-addition of L-NAME, confirming the critical role of NO production (Fig. 6A, lane 11)). Conversely, DMFO, the inhibitor of ornithine decarboxylase (ODC1)—the essential enzyme for polyamine synthesis—did not significantly affect PD-L1 and p-STAT3 levels (Fig. 1A, B, Fig. 6, lane 9). These results suggest that the level of NO, but not the levels of polyamines, regulates STAT3-mediated PD-L1 expression. Interestingly, p-STAT3-expression was concentrated on tumor cells in the regions infiltrated by TAMs in a manner dissimilar to PD-L1 and p-SMAD3 detected throughout the tumor epithelia (Fig. 6B). This is consistent with the report that STAT3 is part of the paracrine signaling pathway between TAMs and breast tumor cells [73].

3.4. Sepiapterin reprograms M2-type TAMs to M1-type TAMs in mammary tumors

Lastly, we tested whether sepiapterin could indeed reprogram M2-type TAMs to M1-type TAMs in mammary tumors, consistent with *in vitro* results (Fig. 2B, Fig. 4A, B). As expected, control tumors showed predominantly CD163 + M2-type TAMs (M1/M2 = 10%). L-NAME further depleted M1-type TAMs (M1/M2 < 1%). Conversely, sepiapterin-treated tumors showed predominantly CD80 + M1-type TAMs (M1/M2 = 90%) (Fig. 7). These results altogether demonstrate that sepiapterin efficiently improves the immunogenicity and suppresses the growth of mammary tumors.

4. Discussion

Recently, the FDA (March 2019) approved the first immunotherapy drug (Atezolizumab, PD-L1 inhibitory antibody) for treating triple-negative breast cancer. This subtype, comprising 10–12% of breast cancers, harbors a higher number of tumor-infiltrating cytotoxic (CD8 +) T cells and is more immuno-stimulatory than other types of breast cancers [2–6]. In contrast, the majority (88–90%) of breast tumors—hormone receptor (ER/PR)-positive and/or HER2-positive types—are mostly immuno-suppressive, harboring a large number of $FoxP3^+$ regulatory T (Treg) cells and a low number of cytotoxic T cells [2–4]. These types of breast cancers only modestly responded to a PD-1-targeting drug (Pembrolizumab) in the earlier clinical trials [1]. Nevertheless, more

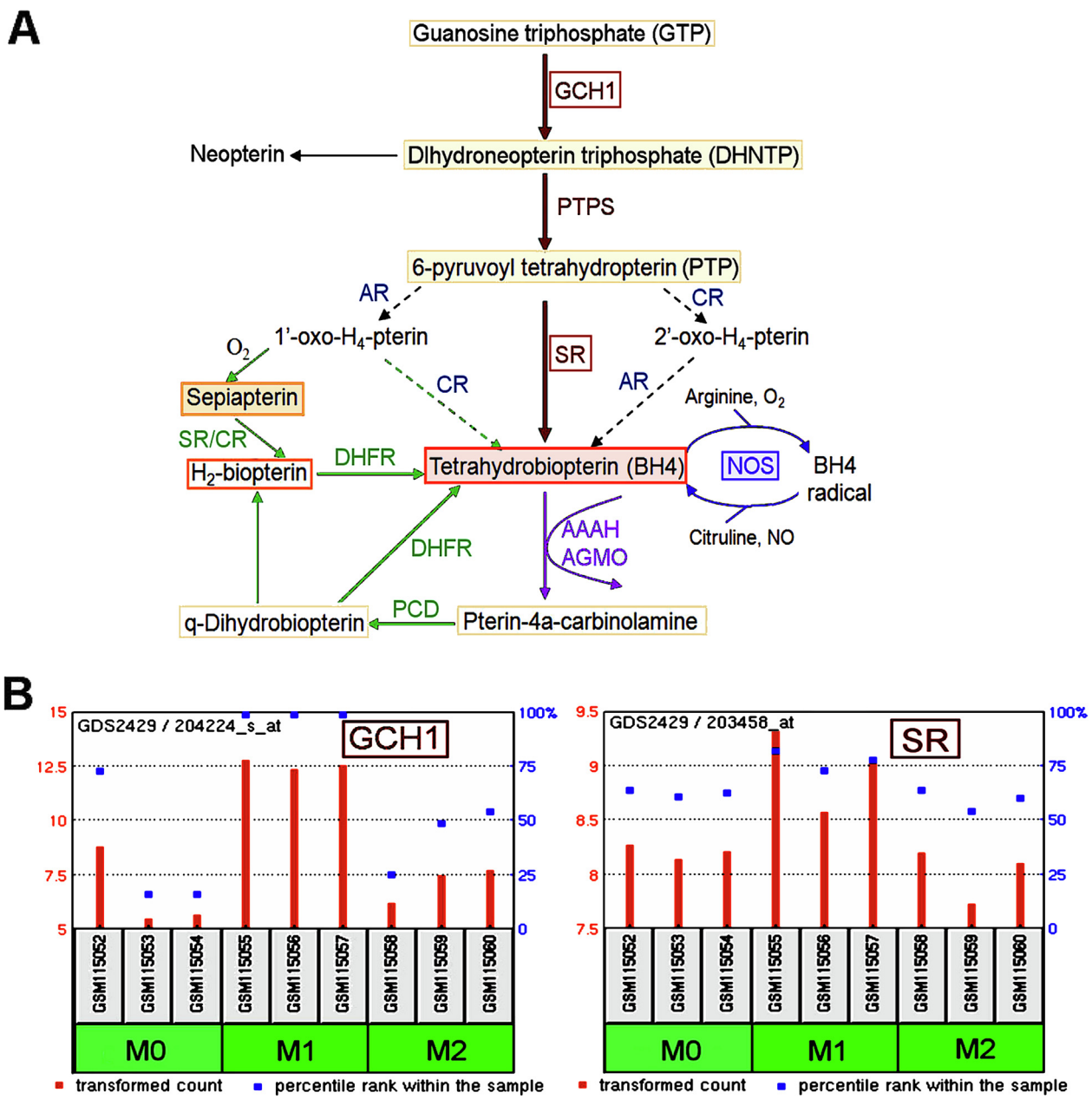

Fig. 3. BH_4 levels are likely to be elevated in M1 and down-modulated in M2 TAMs. A) Schematic of Tetrahydrobiopterin (BH_4) synthesis pathways: De novo biosynthesis (brown) and regeneration (green). Abbreviations: GTPCH, GTP cyclohydrolase I; PTPS, 6-pyruvoyl-tetrahydropterin synthase; SR, sepiapterin reductase; AR, aldose reductase; CR, carbonyl reductase; DHFR, dihydrofolate reductase; DHPR, dihydropteridine reductase; PCD, pterin-4a-carbinol-amine dehydratase; AAAH, aromatic amino acid hydroxylases; AGMO, alkyl-glycerol monooxygenase; NOS, nitric oxide synthase [60]. B) Expression levels of key enzymes for BH_4 synthesis, GTPCH (left) and SR (right), in inactive (M0), M1 or M2 human macrophages (GSE5099) [58].

than half of over 80 ongoing immunotherapy trials for breast cancer are still targeting PD-1/PD-L1 [2,3,5–8]. It is imperative to develop a novel approach to improve the immunogenicity of breast cancer.

In the present study, we tested whether sepiapterin, an endogenous biosynthetic precursor of the NOS cofactor BH_4, could improve the immunogenicity and suppress the growth of mammary tumors using *ex vivo* 3D culture models. We showed that sepiapterin normalized arginine metabolism of both mammary tumor cells and TAMs by elevating the NO-to-polyamine ratio. This was accompanied by downmodulation of the immune checkpoint ligand, PD-L1, in tumor cells; reprogramming of TAMs from the immune-suppressive M2-type to the immunostimulatory M1-type; and growth suppression of mammary tumors (Fig. 7B).

Such effects of sepiapterin were largely due to its suppression of STAT3 (Fig. 6A), a transcription factor that contributes to the immunoevasive phenotype of tumors [74]. STAT3 induces the expression of genes critically involved in immune-suppression, such as PD-L1, IL-10 and TGF-β [70,75,76]. As a mechanism of NO-mediated suppression of STAT3 activity, Kim et al. reported that NO directly S-nitrosylates STAT3 (at Cys259) to inhibit its activation [72]. In support of Kim et al.'s finding, we also observed that a treatment of CA1d breast cancer cells with sepiapterin or L-NAME up- or down-regulated S-nitrosylation levels of STAT3, respectively (data not shown). In fact, S-nitrosylation levels of STAT3 were negatively correlated with the activation (phosphorylation) levels of the protein (Fig. 6A). This suggests that sepiapterin-mediated suppression of STAT3 activity was at least in part mediated by the increase in S-nitrosylation.

Sepiapterin is likely to promote the activities of NOS-1 and -3 in

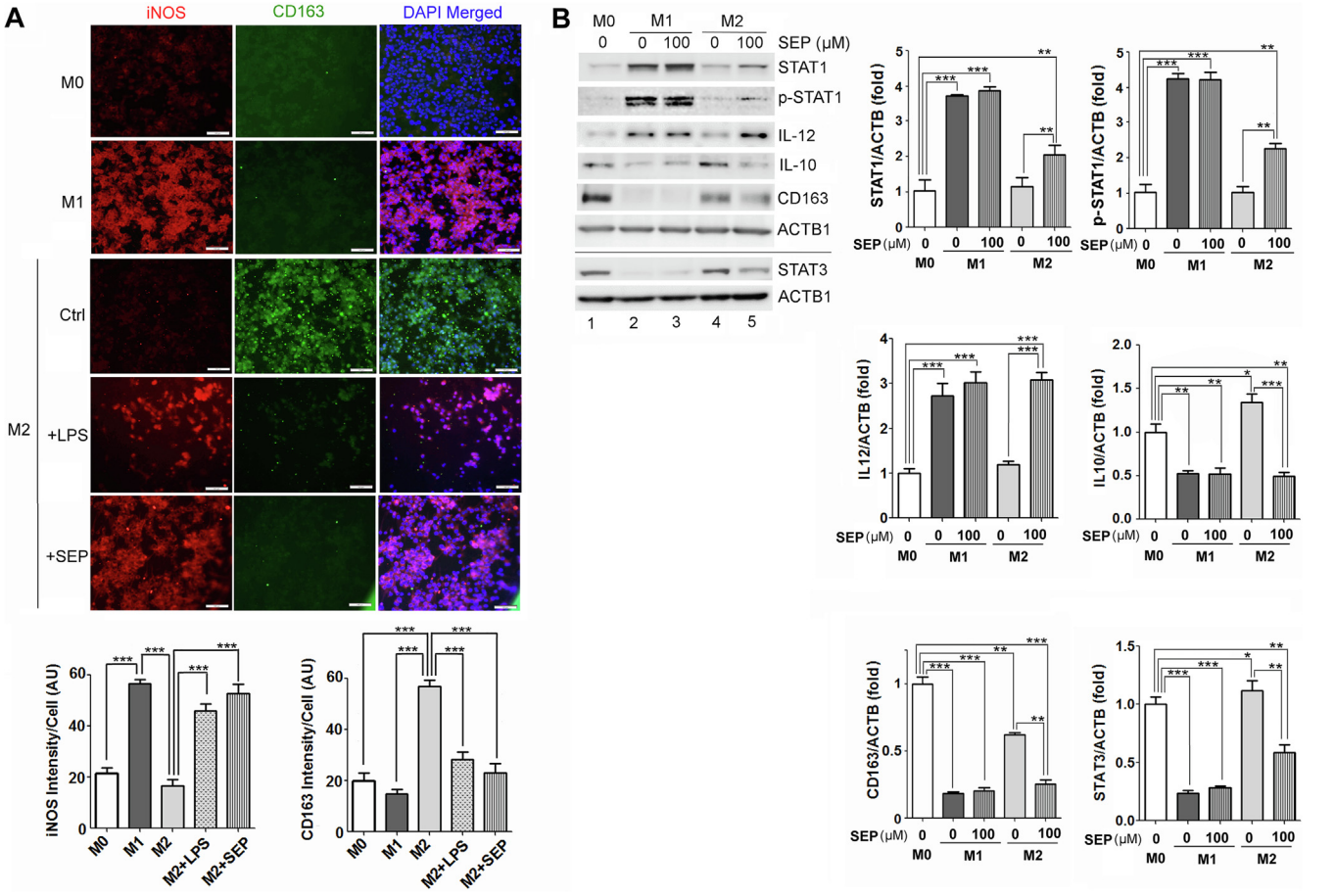

Fig. 4. Sepiapterin induces conversion of M2-type macrophages to M1-type macrophages *in vitro*. A) (Left) THP-1 human macrophages (M0) were *in vitro*- polarized to M1-type (by LPS + INFγ) or M2-type (by IL4 + IL13). M2-type macrophages were further treated with LPS (1 mg/ml, positive control) or sepiapterin (SEP, 100 μM) to test for their conversion to M1-type. M1 marker (red, iNOS [NOS2]); M2 marker (green, CD163). Scale bars: 50 μm. (Right) Quantification of the intensity of NOS2 or CD163 signal per cell. Error bars: ± SEM. ***, p-value < 0.001. B) (Left top) Western blot analysis of THP-1 macrophages in M0, M1 or M2 states and treated with vehicle or SEP as in A). (Right) The blots were analyzed for the expression of STAT1, p-STAT1 (p-Y701), IL-12, IL-10, CD163 or STAT3. β-actin (ACTB1) was used as the internal loading control. The intensity of each blot was quantified, normalized against ACTB1 signal and shown as the fold difference with respect to M0. Error bars: ± SEM. ***, p-value < 0.001, **, p-value < 0.005, and *, p-value < 0.05.

breast cancer cells, and NOS-2 in macrophages. We previously showed that breast epithelial cells express NOS-1 and -3 at high levels, but not NOS-2. Such expression patterns of NOS1-3 in breast cells do not change during cancer progression, despite that the levels of the NOS cofactor, BH_4, (and NO) decline along with malignant progression [39]. This suggests that changes in BH_4 levels have no effect on NOS levels and that supplementing sepiapterin in breast cancer cells would only promote the activities of NOS-1 and -3. Conversely, in macrophages NOS-2 expression is 40–50% higher than NOS-1 and -3, and is further increased in the M1-type [58]. Moreover, we observed that the use of an NOS-2 inhibitor (1400w) along with M1-polarizing agents (LPS and IFNγ) inhibited M1-polarization (increase in NO/polyamine ratio and increase in M1 marker), but instead induced M2-polarization (decrease in NO/polyamine ratio and increase in M2 marker) (data not shown). This result suggests that NOS-2 is essential for M1-polarization of macrophages and, thus, would be involved in sepiapterin-induced M2-to-M1 reprogramming of macrophages.

We showed that sepiapterin effectively shifts arginine metabolism from the pathways synthesizing polyamines to that synthesizing NO in breast cancer cells and macrophages. This is in line with previous reports that elevated NO synthesis inhibits polyamine synthesis and the downstream signaling [22–29,50–54]. Polyamines are polycationic metabolites essential for cell proliferation and immuno-suppression and are elevated in many types of tumors. After their biosynthesis, polyamines are transported through the specific transporters and elicit autocrine/paracrine signaling [22,24,27,28,50]. On one hand, they play critical roles in cell cycle progression, gene transcription, protein translation and oxidative stress, contributing to the proliferative potential of tumor cells [77–79]. On the other hand, polyamines help expand the populations of immuno-suppressive leukocytes within tumors, including myeloid derived suppressor cells (MDSCs), Tregs, and M2-type macrophages. This is partly ascribed to the polyamine-mediated upregulation of CD73 and CD39, ectonucleotidases involved in the production of the immuno-suppressive adenosine [33,80–82]. Extracellular adenosine, which binds its cognate receptors, inhibits T cell signaling, induces the expansion of immuno-suppressive leukocytes and contributes to the activation of PD-L1/PD-1 immune checkpoint pathway [83,84].

Elevated expression of PD-L1 on tumor cells and M2-type macrophages is a major contributor to the immuno-suppressive nature of tumors. PD-L1 binds the receptor, PD-1, on the surface of cytotoxic T cells and inhibits their tumoricidal activity [4,57,85]. Reprogramming of M2-type TAMs (PD-L1-high) to M1-type TAMs (PD-L1-low) has been actively explored as a means to improve the immunogenicity of tumors [86]. However, most studies have tested the application of pro-inflammatory agents (e.g., LPS, IFN-γ, or TNFα) to M2-type macrophages *in vitro* [10,11]. These agents would not only induce adverse systemic toxicity (e.g., septic shock) *in vivo* [13], but also exert both anti- and pro-tumor effects [17,18].

Our results showed that sepiapterin dramatically reprograms M2-

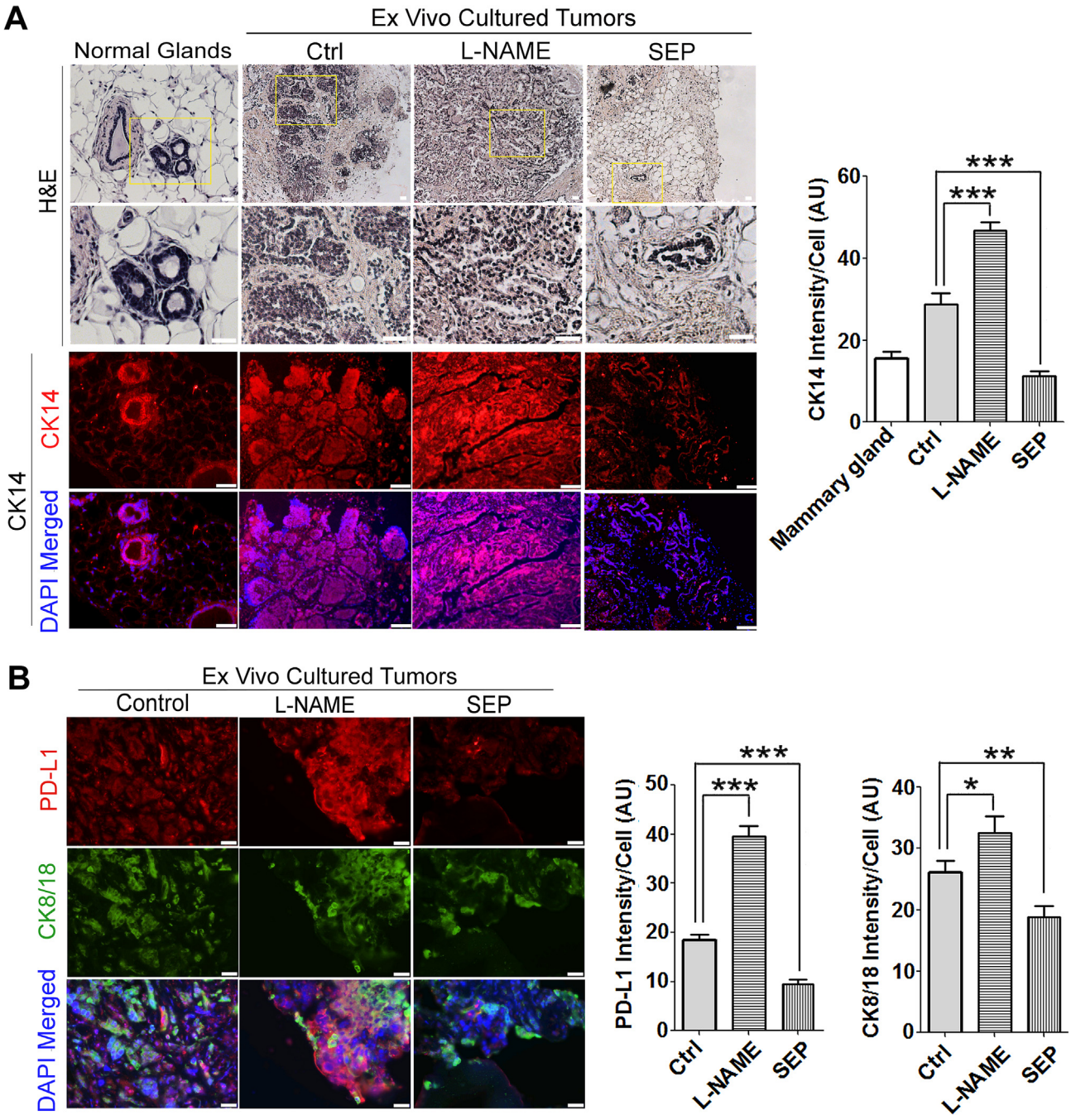

Fig. 5. Sepiapterin induces immuno-stimulatory-shift of mammary tumor cells. A) (Left) Mammary tumors from MMTV-PyMT mice (18 weeks) were *ex vivo* 3D-cultured [45,46] under treatment with vehicle (PBS), L-NAME (2.5 mM, NOS inhibitor) or sepiapterin (100 μM) for 1 week. First column: normal mouse mammary glands. Second, third and fourth columns: *ex vivo*-cultured tumors. First row: 100x (normal glands), 40x (ex vivo tumors); second row: 200x H&E images. Third row: CK14 staining (mammary epithelial marker); fourth row: DAPI-merged. Note the restoration of normal-like gland (from H&E staining) and reduction in the epithelial density (from CK14 staining) by sepiapterin vs. worsened malignancy by L-NAME. Scale bars: 50 μm. (Right) Quantification of the intensity of CK14 signal per cell. Error bars: ± SEM. ***, p-value < 0.001. B) (Left) Mammary tumors from MMTV-PyMT mice were *ex vivo* 3D cultured as in A), paraffin-embedded, sectioned and stained for PD-L1 (red) and CK8/18 (green, mammary epithelial marker). (Right) Quantification of the intensities of PD-L1 and CK8/18 signals per cell. Error bars: ± SEM. *, p-value < 0.05; **, p-value < 0.01, ***, p-value < 0.001.

type TAMs to M1-type TAMs within tumors, suggesting its potential utility as an effective immunotherapy drug. Besides, sepiapterin, an endogenously-produced precursor of BH_4, has been safely utilized in clinical trials for treating patients with phenylketonuria, a metabolic disorder caused by BH_4 deficiency [87]. Our finding is in line with the report that curcumin, the polyphenol component of turmeric, could reprogram M2-type tumor-associated microglia in the brain to M1-type and effectively kill glioblastoma [88]. Furthermore, curcumin is shown to inhibit STAT3 in TAMs in both *in vitro* and *in vivo* conditions, in a manner similar to our results. Polyphenols are plant-derived anti-oxidants and reported to promote NO production by protecting BH_4 from ROS-mediated degradation [89–91]. (Oxidative degradation of BH_4 is a major cause of BH_4 deficiency and NOS dysfunction [36,39].) The findings of our and other studies strongly suggest the utility of normalizing NO production in the immunotherapy of different types of tumors and warrant further investigation of their clinical feasibility.

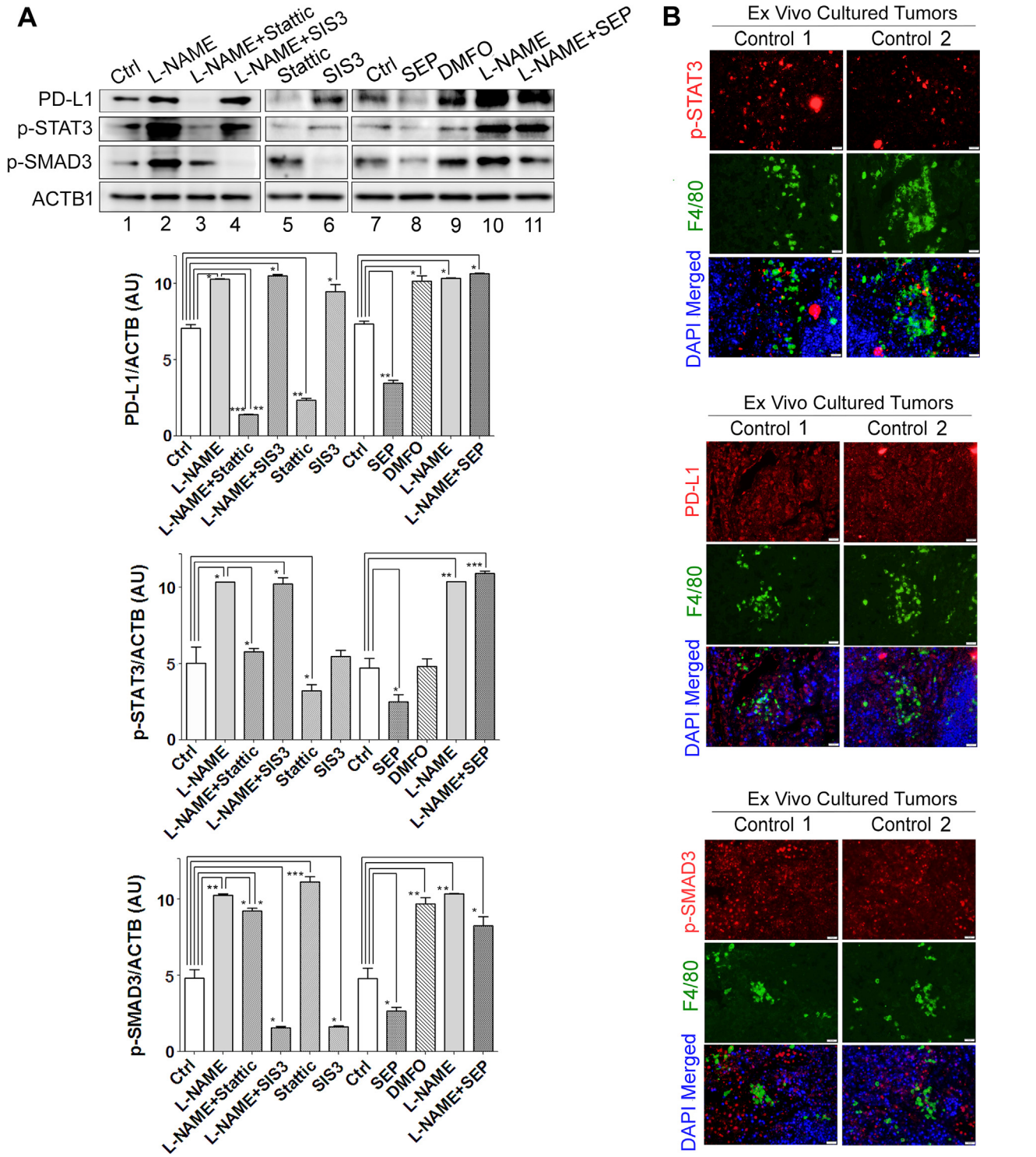

Fig. 6. STAT3 plays critical role in NO-mediated PD-L1 regulation. A) (Top) Western blots of CA1d cells with different treatments: Lane 1: vehicle-treated (Ctrl); lane 2: L-NAME; lane 3: L-NAME + Stattic (STAT3 inhibitor); lane 4: L-NAME + SIS3 (SMAD3 inhibitor); lane 5: Stattic; lane 6: SIS3; lane 7: vehicle-treated (Ctrl); lane 8: Sepiapterin (SEP, 100 μM); lane 9: DMFO (ODC1 inhibitor); lane 10: L-NAME; and lane 11: L-NAME + SEP. Blots were analyzed for the levels of PD-L1, p-STAT3 and p-SMAD3. β-actin (ACTB1) was used as the internal loading control. Note the dramatic decrease of PD-L1 and p-STAT3 levels by L-NAME + Stattic (lane 3), Stattic (lane 5) or SEP treatment (lane 8). (Second, third and fourth panels) Quantification of the intensities of PD-L1, p-STAT3 and p-SMAD3 normalized against ACTB. Error bars: ± SEM. AU, arbitrary unit. *, p-value < 0.05; **, p-value < 0.01, ***, p-value < 0.001. B) Co-staining of p-STAT3, PD-L1 or p-SMAD3 (red) with macrophage marker (F4/80, green). Note the concentrated localization of p-STAT3-expressing tumor cells in the regions infiltrated by macrophages.

CRediT authorship contribution statement

Xunzhen Zheng: Data curation, Formal analysis, Investigation, Methodology. **Veani Fernando:** Data curation, Formal analysis, Investigation, Visualization. **Vandana Sharma:** Data curation, Formal analysis, Investigation, Writing - original draft, Writing - review & editing. **Yashna Walia:** Investigation, Methodology, Resources. **Joshua Letson:** Investigation, Methodology. **Saori Furuta:** Conceptualization,

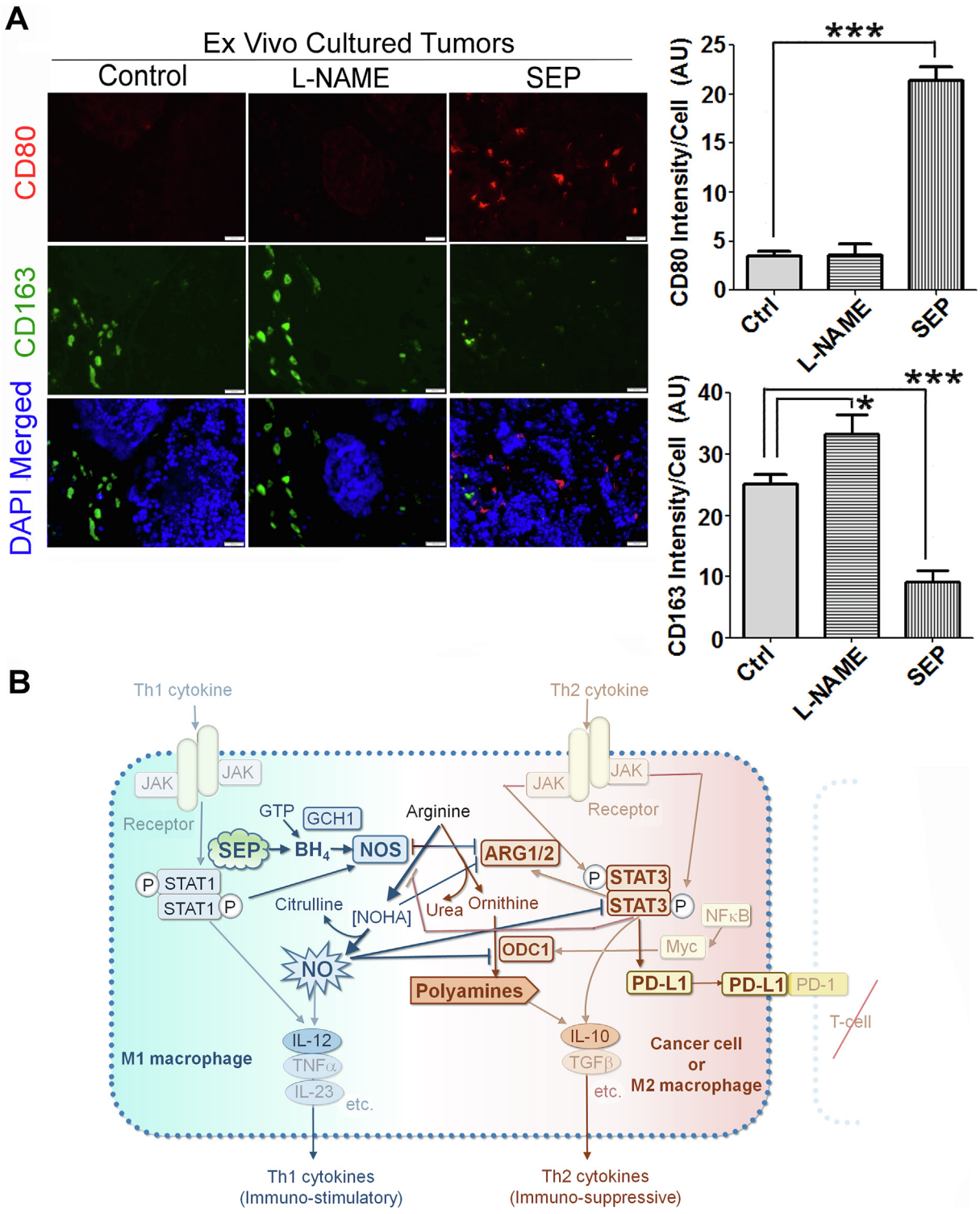

Fig. 7. Sepiapterin reprograms M2-type TAMs to M1-type TAMs in mammary tumors. A) (Left) Mammary tumors from MMTV-PyMT mice were *ex vivo*-cultured as in Fig. 5A, paraffin-embedded, sectioned and co-stained for M1/M2 macrophage markers: CD80 (M1, red) vs. CD163 (M2, green). Counter-stained with DAPI. Note the prominent M2-type macrophages (green) in control and L-NAME-treated tumors vs. prominent M1-type macrophages (red) in SEP-treated tumor. Scale bars: 50 μm. (Right) Quantification of the intensity of CD80 or CD163 signal per cell. Error bars: ± SEM. *, p-value < 0.05, ***, p-value < 0.001. B) Scheme of signaling pathways ivolved in sepiapterin-mediated immuno-stimulatory shift of macrophage and cancer cell.

Data curation, Formal analysis, Funding acquisition, Investigation, Methodology, Project administration, Resources, Supervision, Writing - original draft, Writing - review & editing.

Declaration of Competing Interest

The authors declare that the research was conducted in the absence of any commercial or financial relationships that could be construed as a potential conflict of interest.

Acknowledgement

We thank Dr. Kam Yeung and Christopher Figy for providing us with MMTV-PyMT mammary tumors; Allen Schroering (Histology Core, UT) for preparation of histological samples; Dr. David Weaver (FACS/imaging core, UT) for fluorometric measurement; and Caoqinglong Huang (Department of Cancer Biology, UT) for the preliminary study of THP-1 polarization/remodeling. This work was supported by the Startup Fund from University of Toledo Health Science Campus, College of Medicine and Life Sciences, Department of Cancer Biology to S.F.; Ohio Cancer Research Grant (Project #: 5017) to S.F; Medical Research Society (Toledo Foundation) Award to S.F; and American Cancer Society Research Scholar Grant (RSG-18-238-01-CSM) to S.F.

References

[1] N.M. Ayoub, K.M. Al-Shami, R.J. Yaghan, Immunotherapy for HER2-positive breast cancer: recent advances and combination therapeutic approaches, Breast Cancer (Dove Med Press) 11 (2019) 53–69.
[2] R.M. Neve, K. Chin, J. Fridlyand, J. Yeh, F.L. Baehner, T. Fevr, L. Clark, N. Bayani, J.-P. Coppe, F. Tong, T. Speed, P.T. Spellman, S. DeVries, A. Lapuk, N.J. Wang, W.-L. Kuo, J.L. Stilwell, D. Pinkel, D.G. Albertson, F.M. Waldman, F. McCormick, R.B. Dickson, M.D. Johnson, M. Lippman, S. Ethier, A. Gazdar, J.W. Gray, A collection of breast cancer cell lines for the study of functionally distinct cancer subtypes, Cancer Cell 10 (6) (2006) 515–527.
[3] American Cancer Society. Breast Cancer Facts & Figures 2017–2018, 2017.
[4] M.D. Wellenstein, K.E. de Visser, Cancer-cell-intrinsic mechanisms shaping the tumor immune landscape, Immunity 48 (3) (2018) 399–416.
[5] M. Liu, F. Guo, Recent updates on cancer immunotherapy, Precis. Clin. Med. 1 (2) (2018) 65–74.
[6] F.S. Cyprian, S. Akhtar, Z. Gatalica, S. Vranic, Targeted immunotherapy with a checkpoint inhibitor in combination with chemotherapy: A new clinical paradigm in the treatment of triple-negative breast cancer, Bosn. J. Basic Med. Sci. 19 (3) (2019) 227–233.
[7] I. Makhoul, M. Atiq, A. Alwbari, T. Kieber-Emmons, Breast Cancer Immunotherapy: An Update, Breast Cancer (Auckl) 12 (2018) 1178223418774802.
[8] Curr Surg Rep 5 (12) (2017), https://doi.org/10.1007/s40137-017-0194-1.
[9] A. Mantovani, F. Marchesi, A. Malesci, L. Laghi, P. Allavena, Tumour-associated macrophages as treatment targets in oncology, Nat. Rev. Clin. Oncol. 14 (7) (2017) 399–416.
[10] D. Duluc, M. Corvaisier, S. Blanchard, L. Catala, P. Descamps, E. Gamelin, S. Ponsoda, Y. Delneste, M. Hebbar, P. Jeannin, Interferon-γ reverses the immunosuppressive and protumoral properties and prevents the generation of human tumor-associated macrophages, Int. J. Cancer 125 (2) (2009) 367–373.
[11] S.V. Kalish, S.V. Lyamina, E.A. Usanova, E.B. Manukhina, N.P. Larionov, I.Y. Malyshev, Macrophages reprogrammed in vitro towards the M1 phenotype and activated with LPS extend lifespan of mice with ehrlich ascites carcinoma, Med. Sci. Monit. Basic Res. 21 (2015) 226–234.
[12] S. Adams, Toll-like receptor agonists in cancer therapy, Immunotherapy 1 (6) (2009) 949–964.
[13] L. Faulkner, A. Cooper, C. Fantino, D.M. Altmann, S. Sriskandan, The mechanism of superantigen-mediated toxic shock: not a simple Th1 cytokine storm, J. Immunol. 175 (10) (2005) 6870–6877.
[14] J. Ishihara, A. Ishihara, L. Potin, P. Hosseinchi, K. Fukunaga, M. Damo, T.F. Gajewski, M.A. Swartz, J.A. Hubbell, Improving efficacy and safety of agonistic anti-CD40 antibody through extracellular matrix affinity, Mol. Cancer Ther. 17 (11) (2018) 2399–2411.
[15] B.J. Ignacio, T.J. Albin, A.P. Esser-Kahn, M. Verdoes, Toll-like receptor agonist conjugation: a chemical perspective, Bioconjug. Chem. 29 (3) (2018) 587–603.
[16] K. Iribarren, N. Bloy, A. Buqué, I. Cremer, A. Eggermont, W.H. Fridman, J. Fucikova, J. Galon, R. Špíšek, L. Zitvogel, G. Kroemer, L. Galluzzi, Trial Watch: immunostimulation with Toll-like receptor agonists in cancer therapy, Oncoimmunology 5 (3) (2015) e1088631-e1088631.
[17] X. Wang, Y. Lin, Tumor necrosis factor and cancer, buddies or foes? Acta Pharmacol. Sin. 29 (11) (2008) 1275–1288.
[18] M. Mojic, K. Takeda, Y. Hayakawa, The dark side of IFN-γ: its role in promoting cancer immunoevasion, Int J Mol Sci 19(1) pii (2017) E89.
[19] J.P. Pradere, D.H. Dapito, R.F. Schwabe, The Yin and Yang of toll-like receptors in cancer, Oncogene 33 (27) (2014) 3485–3495.
[20] G. Murugaiyan, R. Agrawal, G.C. Mishra, D. Mitra, B. Saha, Functional dichotomy in CD40 reciprocally regulates effector T cell functions, J. Immunol. 177 (10) (2006) 6642–6649.
[21] K. Kus, A. Kij, A. Zakrzewska, A. Jasztal, M. Stojak, M. Walczak, S. Chlopicki, Alterations in arginine and energy metabolism, structural and signalling lipids in metastatic breast cancer in mice detected in plasma by targeted metabolomics and lipidomics, Breast Cancer Res. 20 (1) (2018) 148.
[22] H. Tapiero, G. Mathé, P. Couvreur, K.D. Tew, I. Arginine, Biomed. Pharmacother. 56 (9) (2002) 439–445.
[23] Dis. Model. Mech. 11 (8) (2018) dmm033332, https://doi.org/10.1242/dmm.033332.
[24] M. Gogoi, A. Datey, K.T. Wilson, D. Chakravortty, Dual role of arginine metabolism in establishing pathogenesis, Curr. Opin. Microbiol. 29 (2016) 43–48.
[25] J.P. Tenu, M. Lepoivre, C. Moali, M. Brollo, D. Mansuy, J.L. Boucher, Effects of the new arginase inhibitor N(omega)-hydroxy-nor-L-arginine on NO synthase activity in murine macrophages, Nitric Oxide 3 (6) (1999) 427–438.
[26] S.W. Park, L.N. Wei, Regulation of c-myc gene by nitric oxide via inactivating NF-κB complex in P19 mouse embryonal carcinoma cells, J. Biol. Chem. 278 (2003) 29776.
[27] M.D. Hogarty, M.D. Norris, K. Davis, X. Liu, N.F. Evageliou, C.S. Hayes, B. Pawel, R. Guo, H. Zhao, E. Sekyere, J. Keating, W. Thomas, N.C. Cheng, J. Murray, J. Smith, R. Sutton, N. Venn, W.B. London, A. Buxton, S.K. Gilmour, G.M. Marshall, M. Haber, ODC1 is a critical determinant of MYCN oncogenesis and a therapeutic target in neuroblastoma, Cancer Res. 68 (23) (2008) 9735–9745.
[28] A.S. Bachmann, D. Geerts, Polyamine synthesis as a target of MYC oncogenes, J. Biol. Chem. 293 (48) (2018) 18757–18769.
[29] P.M. Bauer, G.M. Buga, J.M. Fukuto, A.E. Pegg, L.J. Ignarro, Nitric oxide inhibits ornithine decarboxylase via S-nitrosylation of cysteine 360 in the active site of the enzyme, J. Biol. Chem. 276 (37) (2001) 34458–34464.
[30] N. Shah, T. Thomas, A. Shirahata, L.H. Sigal, T.J. Thomas, Activation of nuclear factor kappaB by polyamines in breast cancer cells, Biochemistry 38 (45) (1999) 14763–14774.
[31] T. Thomas, T.J. Thomas, Polyamine metabolism and cancer, J. Cell Mol. Med. 7 (2) (2003) 113–126.
[32] C.S. Hayes, A.C. Shicora, M.P. Keough, A.E. Snook, M.R. Burns, S.K. Gilmour, Polyamine-blocking therapy reverses immunosuppression in the tumor microenvironment, Cancer Immunol Res. 2 (3) (2014) 274–285.
[33] E.T. Alexander, A. Minton, M.C. Peters, O.t. Phanstiel, S.K. Gilmour, A novel polyamine blockade therapy activates an anti-tumor immune response, Oncotarget 8 (48) (2017) 84140–84152.
[34] U. Förstermann, W.C. Sessa, Nitric oxide synthases: regulation and function, Eur. Hear J. 33 (7) (2012) 829–837.
[35] A.L. Moens, D.A. Kass, Tetrahydrobiopterin and cardiovascular disease, Arterioscler. Thromb. Vasc. Biol. 26 (11) (2006) 2439–2444.
[36] V. Fernando, X. Zheng, Y. Walia, V. Sharma, J. Letson, S. Furuta, S-Nitrosylation: An Emerging Paradigm of Redox Signaling, Antioxidants (Basel) 8(9) (2019) pii: E404.
[37] S. Furuta, G. Ren, J. Mao, M.J. Bissell, Laminin signals initiate the reciprocal loop that informs breast-specific gene expression and homeostasis by activating NO, p53 and microRNA, Elife 7 (2018) e26148.
[38] B.L. Ricca, G. Venugopalan, S. Furuta, K. Tanner, W.A. Orellana, C.D. Reber, D.G. Brownfield, M.J. Bissell, D.A. Fletcher, Transient external force induces phenotypic reversion of malignant epithelial structures via nitric oxide signaling, Elife 7 (2018) e26161.
[39] G. Ren, X. Zheng, M. Bommarito, S. Metzger, J. Letson, Y. Walia, S. Furuta, Reduced basal nitric oxide production induces precancerous mammary lesions via ERBB2 and TGFβ, Sci. Rep. 9 (1) (2019) 6688.
[40] B. Pigott, K. Bartus, J. Garthwaite, On the selectivity of neuronal NOS inhibitors, Br. J. Pharmacol. 168 (5) (2013) 1255–1265.
[41] S.J. Santner, P.J. Dawson, L. Tait, H.D. Soule, J. Eliason, A.N. Mohamed, S.R. Wolman, G.H. Heppner, F.R. Miller, Malignant MCF10CA1 cell lines derived from premalignant human breast epithelial MCF10AT cells, Breast Cancer Res. Treat. 65 (2) (2001) 101–110.
[42] S. Tsuchiya, M. Yamabe, Y. Yamaguchi, Y. Kobayashi, T. Konno, K. Tada, Establishment and characterization of a human acute monocytic leukemia cell line (THP-1), Int. J. Cancer 26 (2) (1980) 171–176.
[43] M.P. Smith, H. Young, A. Hurlstone, C. Wellbrock, Differentiation of THP1 cells into macrophages for transwell co-culture assay with melanoma cells, Bio Protoc. 5 (21) (2015) e1638.
[44] C. Li, M. Levin, D.L. Kaplan, Bioelectric modulation of macrophage polarization, Sci. Rep. 6 (2016) 21044.
[45] J.C. Grivel, L. Margolis, Use of human tissue explants to study human infectious agents, Nat. Protoc. 4 (2) (2009) 256–269.
[46] Curr. Protocols Pharmacol. 60 (1) (2013), https://doi.org/10.1002/0471141755.2013.60.issue-110.1002/0471141755.ph1423s60.
[47] P.A. Vidi, M.J. Bissell, S.A. Lelièvre, Three-dimensional culture of human breast epithelial cells: the how and the why, Methods Mol. Biol. 945 (193–219) (2013).
[48] Bio-Protocol 9 (19) (2019), https://doi.org/10.21769/BioProtoc.3392.
[49] S.-Y. Lee, R. Meier, S. Furuta, M.E. Lenburg, P.A. Kenny, R. Xu, M.J. Bissell, FAM83A confers EGFR-TKI resistance in breast cancer cells and in mice, J. Clin. Invest. 122 (2012) 3211–3220.
[50] E. Muraille, O. Leo, M. Moser, TH1/TH2 paradigm extended: macrophage polarization as an unappreciated pathogen-driven escape mechanism? Front. Immunol. 6 (2014) 603.
[51] R. Singh, S. Pervin, A. Karimi, S. Cederbaum, G. Chaudhuri, Arginase activity in human breast cancer cell lines: N(omega)-hydroxy-L-arginine selectively inhibits cell proliferation and induces apoptosis in MDA-MB-468 cells, Cancer Res. 60 (12) (2000) 3305–3312.
[52] M. Hecker, H. Nematollahi, C. Hey, R. Busse, K. Racké, Inhibition of arginase by NG-hydroxy-L-arginine in alveolar macrophages: implications for the utilization of L-arginine for nitric oxide synthesis, FEBS Lett. 359 (2–3) (1995) 251–254.
[53] F. Daghigh, J.M. Fukuto, D.E. Ash, Inhibition of rat liver arginase by an intermediate in NO biosynthesis, NG-hydroxy-L-arginine: implications for the regulation of nitric oxide biosynthesis by arginase, Biochem. Biophys. Res. Commun. 202 (1) (1994) 174–180.
[54] R. Singh, S. Pervin, G. Chaudhuri, Caspase-8-mediated BID cleavage and release of mitochondrial cytochrome c duringN ω-hydroxy-l-arginine-induced apoptosis in MDA-MB-468 Cells: ANTAGONISTIC EFFECTS OF l-ORNITHINE, J. Biol. Chem. 277 (40) (2002) 37630–37636.

[55] K. Singh, L.A. Coburn, M. Asim, D.P. Barry, M.M. Allaman, C. Shi, M.K. Washington, P.B. Luis, C. Schneider, A.G. Delgado, M.B. Piazuelo, J.L. Cleveland, A.P. Gobert, K.T. Wilson, Ornithine decarboxylase in macrophages exacerbates colitis and promotes colitis-associated colon carcinogenesis by impairing M1 immune responses, Cancer Res. 78 (15) (2018) 4303–4315.

[56] M. Rath, I. Müller, P. Kropf, E.I. Closs, M. Munder, Metabolism via arginase or nitric oxide synthase: two competing arginine pathways in macrophages, Front. Immunol. 5 (2014) 532.

[57] Immunology 155 (3) (2018) 285–293, https://doi.org/10.1111/imm.2018.155.issue-3.

[58] G. Solinas, S. Schiarea, M. Liguori, M. Fabbri, S. Pesce, L. Zammataro, F. Pasqualini, M. Nebuloni, C. Chiabrando, A. Mantovani, P. Allavena, Tumor-conditioned macrophages secrete migration-stimulating factor: a new marker for M2-polarization, influencing tumor cell motility, J. Immunol. 185 (1) (2010) 642–652.

[59] G. Werner-Felmayer, G. Golderer, E.R. Werner, Tetrahydrobiopterin biosynthesis, utilization and pharmacological effects, Curr. Drug Metab. 3 (2) (2002) 159–173.

[60] H.L. Kim, Y.S. Park, Maintenance of cellular tetrahydrobiopterin homeostasis, BMB Rep. 43 (9) (2010) 584–592.

[61] C.A. Nichol, C.L. Lee, M.P. Edelstein, J.Y. Chao, D.S. Duch, Biosynthesis of tetrahydrobiopterin by de novo and salvage pathways in adrenal medulla extracts, mammalian cell cultures, and rat brain in vivo, Proc. Natl. Acad. Sci. U.S.A. 80 (6) (1983) 1546–1550.

[62] K. Watschinger, M.A. Keller, E. McNeill, M.T. Alam, S. Lai, S. Sailer, V. Rauch, J. Patel, A. Hermetter, G. Golderer, S. Geley, G. Werner-Felmayer, R.S. Plumb, G. Astarita, M. Ralser, K.M. Channon, E.R. Werner, Tetrahydrobiopterin and alkylglycerol monooxygenase substantially alter the murine macrophage lipidome, Proc. Natl. Acad. Sci. U.S.A. 112 (8) (2015) 2431–2436.

[63] G. Douglas, A.B. Hale, J. Patel, S. Chuaiphichai, A. Al Haj Zen, V.S. Rashbrook, L. Trelfa, M.J. Crabtree, E. McNeill, K.M. Channon, Roles for endothelial cell and macrophage Gch1 and tetrahydrobiopterin in atherosclerosis progression, Cardiovasc. Res. 114 (10) (2018) 1385–1399.

[64] F.O. Martinez, S. Gordon, M. Locati, A. Mantovani, Transcriptional profiling of the human monocyte-to-macrophage differentiation and polarization: new molecules and patterns of gene expression, J. Immunol. 177 (10) (2006) 7303–7311.

[65] X. Cai, Y. Yin, N. Li, D. Zhu, J. Zhang, C.Y. Zhang, K. Zen, Re-polarization of tumor-associated macrophages to pro-inflammatory M1 macrophages by microRNA-155, J. Mol. Cell. Biol. 4 (5) (2012) 341–343.

[66] X. Ma, W. Yan, H. Zheng, Q. Du, L. Zhang, Y. Ban, N. Li, F. Wei, Regulation of IL-10 and IL-12 production and function in macrophages and dendritic cells [version 1; peer review: 3 approved], F1000Research 4(1465) (2015).

[67] J.M. Hu, K. Liu, J.H. Liu, X.L. Jiang, X.L. Wang, Y.Z. Chen, S.G. Li, H. Zou, L.J. Pang, C.X. Liu, X.B. Cui, L. Yang, J. Zhao, X.H. Shen, J.F. Jiang, W.H. Liang, X.L. Yuan, F. Li, CD163 as a marker of M2 macrophage, contribute to predicte aggressiveness and prognosis of Kazakh esophageal squamous cell carcinoma, Oncotarget 8 (13) (2017) 21526–21538.

[68] D.P. Hollern, E.R. Andrechek, A genomic analysis of mouse models of breast cancer reveals molecular features of mouse models and relationships to human breast cancer, Breast Cancer Res. 16 (3) (2014) R59.

[69] F.K. Dermani, P. Samadi, G. Rahmani, A.K. Kohlan, R. Najafi, PD-1/PD-L1 immune checkpoint: potential target for cancer therapy, J. Cell. Physiol. 234 (2) (2019) 1313–1325.

[70] T.L. Song, M.-L. Nairismägi, Y. Laurensia, J.-Q. Lim, J. Tan, Z.-M. Li, W.-L. Pang, A. Kizhakeyil, G.-C. Wijaya, D.-C. Huang, S. Nagarajan, B.K.-H. Chia, D. Cheah, Y.-H. Liu, F. Zhang, H.-L. Rao, T. Tang, E.K.-Y. Wong, J.-X. Bei, J. Iqbal, N.-F. Grigoropoulos, S.-B. Ng, W.-J. Chng, B.-T. Teh, S.-Y. Tan, N.K. Verma, H. Fan, S.-T. Lim, C.-K. Ong, Oncogenic activation of the STAT3 pathway drives PD-L1 expression in natural killer/T-cell lymphoma, Blood 132 (11) (2018) 1146–1158.

[71] B.V. Park, Z.T. Freeman, A. Ghasemzadeh, M.A. Chattergoon, A. Rutebemberwa, J. Steigner, M.E. Winter, T.V. Huynh, S.M. Sebald, S.J. Lee, F. Pan, D.M. Pardoll, A.L. Cox, TGFβ1-mediated SMAD3 enhances PD-1 expression on antigen-specific T cells in cancer, Cancer Discov. 6 (12) (2016) 1366–1381.

[72] J. Kim, J.S. Won, A.K. Singh, A.K. Sharma, I. Singh, STAT3 regulation by S-nitrosylation: implication for inflammatory disease, Antioxid. Redox Signal. 20 (16) (2014) 2514–2527.

[73] J. Yang, D. Liao, C. Chen, Y. Liu, T.H. Chuang, R. Xiang, D. Markowitz, R.A. Reisfeld, Y. Luo, Tumor-associated macrophages regulate murine breast cancer stem cells through a novel paracrine EGFR/Stat3/Sox-2 signaling pathway, Stem Cells 31 (2) (2013) 244–258.

[74] L.M. Jones, M.L. Broz, J.J. Ranger, J. Ozcelik, R. Ahn, D. Zuo, J. Ursini-Siegel, M.T. Hallett, M. Krummel, W.J. Muller, STAT3 establishes an immunosuppressive microenvironment during the early stages of breast carcinogenesis to promote tumor growth and metastasis, Cancer Res. 76 (6) (2016) 1416–1428.

[75] C.M. Hedrich, T. Rauen, S.A. Apostolidis, A.P. Grammatikos, N. Rodriguez Rodriguez, C. Ioannidis, V.C. Kyttaris, J.C. Crispin, G.C. Tsokos, Stat3 promotes IL-10 expression in lupus T cells through < em > trans- < /em > activation and chromatin remodeling, Proceedings of the National Academy of Sciences 111(37) (2014) 13457-13462.

[76] C. Li, A. Iness, J. Yoon, J.R. Grider, K.S. Murthy, J.M. Kellum, J.F. Kuemmerle, Noncanonical STAT3 activation regulates excess TGF-β1 and collagen I expression in muscle of stricturing Crohn's disease, J. Immunol. 194 (7) (2015) 3422–3431.

[77] T. Thomas, T.J. Thomas, Polyamines in cell growth and cell death: molecular mechanisms and therapeutic applications, Cell. Mol. Life Sci. CMLS 58 (2) (2001) 244–258.

[78] R.A. Casero, T. Murray Stewart, A.E. Pegg, Polyamine metabolism and cancer: treatments, challenges and opportunities, Nat. Rev. Cancer 18 (11) (2018) 681–695.

[79] E.W. Gerner, F.L. Meyskens, Polyamines and cancer: old molecules, new understanding, Nat. Rev. Cancer 4 (10) (2004) 781–792.

[80] C. Ye, Z. Geng, D. Dominguez, S. Chen, J. Fan, L. Qin, A. Long, Y. Zhang, T.M. Kuzel, B. Zhang, Targeting ornithine decarboxylase by α-difluoromethylornithine inhibits tumor growth by impairing myeloid-derived suppressor cells, J. Immunol. 196 (2) (2016) 915–923.

[81] B. Allard, M.S. Longhi, S.C. Robson, J. Stagg, The ectonucleotidases CD39 and CD73: novel checkpoint inhibitor targets, Immunol. Rev. 276 (1) (2017) 121–144.

[82] N. Kamatani, D.A. Carson, Dependence of adenine production upon polyamine synthesis in cultured human lymphoblasts, BBA 675 (3–4) (1981) 344–350.

[83] R.D. Leone, L.A. Emens, Targeting adenosine for cancer immunotherapy, J. Immunother. Cancer 6 (1) (2018) 57-57.

[84] B. Allard, S. Pommey, M.J. Smyth, J. Stagg, Targeting CD73 enhances the antitumor activity of anti-PD-1 and anti-CTLA-4 mAbs, Clin. Cancer Res. 19 (20) (2013) 5626–5635.

[85] R.H. Vonderheide, S.M. Domchek, A.S. Clark, Immunotherapy for breast cancer: what are we missing? Clin. Cancer Res. 23 (11) (2017) 2640–2646.

[86] P. Dhupkar, N. Gordon, J. Stewart, E.S. Kleinerman, Anti-PD-1 therapy redirects macrophages from an M2 to an M1 phenotype inducing regression of OS lung metastases, Cancer Med. 7 (6) (2018) 2654–2664.

[87] N. Smith, N. Longo, K. Levert, K. Hyland, N. Blau, Phase I clinical evaluation of CNSA-001 (sepiapterin), a novel pharmacological treatment for phenylketonuria and tetrahydrobiopterin deficiencies, in healthy volunteers, Mol. Genet. Metab. 126 (4) (2019) 406–412.

[88] S. Mukherjee, J. Baidoo, A. Fried, D. Atwi, S. Dolai, J. Boockvar, M. Symons, R. Ruggieri, K. Raja, P. Banerjee, Curcumin changes the polarity of tumor-associated microglia and eliminates glioblastoma, Int. J. Cancer 139 (12) (2016) 2838–2849.

[89] K.B. Pandey, S.I. Rizvi, Plant polyphenols as dietary antioxidants in human health and disease, Oxid. Med. Cell Longev. 2 (5) (2009) 270–278.

[90] J.H. Kim, C. Auger, V. Schini-Kerth, Activation of eNOS by polyphenol-rich products and polyphenolic compounds, Curr. Pharm. Des. 20 (22) (2014) 3521–3529.

[91] R. Furuuchi, I. Shimizu, Y. Yoshida, Y. Hayashi, R. Ikegami, M. Suda, G. Katsuumi, T. Wakasugi, M. Nakao, T. Minamino, Boysenberry polyphenol inhibits endothelial dysfunction and improves vascular health, PLoS ONE 13 (8) (2018) e0202051.